

Experimental Study on Local Heat Transfer Characteristics of Refrigerant R410A Condensing in a Multi-Port Extruded Tube

Xuesong WU^{*1}, Shigeru KOYAMA^{*1}, Ken KUWAHARA^{*1}

E-mail of corresponding author: *koyama@cm.kyushu-u.ac.jp*

(Received 30 October 2007)

In the present study, the local heat transfer characteristics are investigated experimentally for the condensation of a refrigerant R410A in a multi-port tube made of aluminum, which has 12 channels of 681.0 mm in length; 1.12 mm in hydraulic diameter. The tube-wall heat fluxes are measured in each subsection of 75mm in effective cooling length; the wall temperatures are also measured at 8 positions of each side of test-tube. The refrigerant pressure drops in 8 subsections are calculated with the measured pressures at inlet and outlet of the tube. The experiments are carried out with a mass velocity of $G=100\sim 300$ kg/(m²s) and a constant inlet pressure of around 2.50 MPa. The experimental data of pressure drop are compared with the correlation of Koyama et al.[1] correlation (2002), and local heat transfer coefficients are also compared with some correlations.

Key words: *R410A, Multi-port tube, Condensation, Heat transfer*

1. Introduction

Recently environmental protection is taken more attention, inasmuch as the greenhouse effect, desertification and other climate impacts have become serious. In the field of air-conditioning and refrigeration, it is urgently necessary to introduce environment-friendly refrigerants and improve further the performance in the air-conditioning and refrigeration systems in order to reduce the energy consumption. To improve the system performance, the utilization of mini-channel heat transfer tubes in condenser /evaporator is much significant.

There are a few studies on the condensing heat transfer of refrigerants in small diameter tubes. Yang and Webb[2] (1996) carried out experiments on the heat transfer of R12 in a horizontal multi-port extruded tube of 2.64mm in hydraulic diameter and a horizontal multi-port extruded fin tube of 1.56mm in hydraulic diameter. Katsuta[3] (1994) carried out experiments of R134a in several multi-port extruded tubes, and compared the local heat transfer characteristics with several correlations proposed for large diameter tubes. Moser et al. [4] (1998) proposed a correlation using the equivalent Reynolds

number model, based on experimental data of heat transfer in many kinds of horizontal tubes of 4.57-12.7mm I.D. Koyama et al.[1] (2002) experimentally investigated on local characteristics of pressure drop and heat transfer of pure refrigerant R134a condensing in two kinds of multi-port extruded tubes made of aluminum. One has 8 channels of 1.11 mm in hydraulic diameter and another has 19 channels of 0.80 mm in hydraulic diameter. The experimental data of frictional pressure drop and local heat transfer are compared with correlations proposed by other researchers, respectively.

However, it is quite difficult to measure accurately the local heat transfer characteristics of a mini-channel heat transfer tube. More researching efforts are required to investigate the condensation process in a small diameter tube.

In the present study, the local heat transfer of refrigerant R410A condensing in horizontal multi-port extruded tubes of 1.12mm in hydraulic diameter are investigated experimentally.

2. Experimental apparatus and data

^{*1} Interdisciplinary Graduate School of Engineering Sciences

reduction

2.1 Experimental Apparatus and experimental conditions

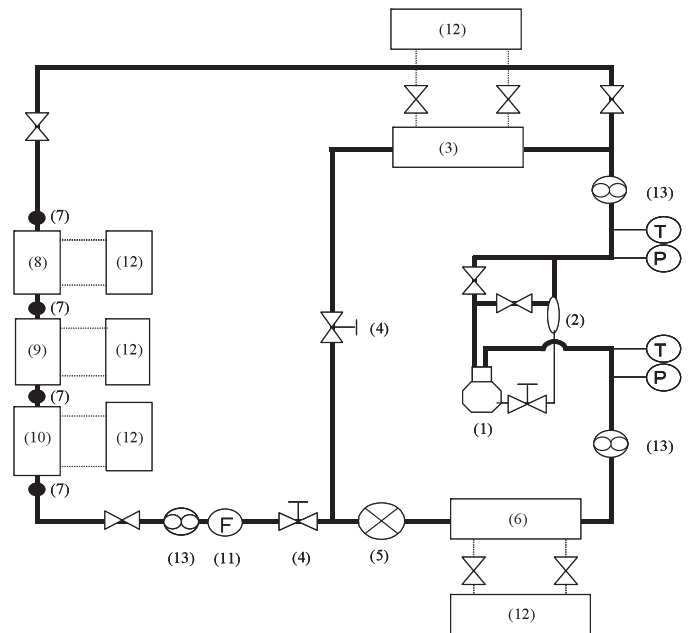
Figure 1 shows the schematic diagram of the experimental apparatus employed in present study. The apparatus is composed mainly of a compressor (1), a condenser (3), a flow control valve (4), an expansion valve (5), an evaporator (6), a test section (9), and 5 constant temperature water circulators (12).

The refrigerant discharged from a compressor (1) flows into both the main loop and the bypass loop. In the main loop, the refrigerant flows into a pre-cooler (8) for controlling the inlet superheat. Refrigerant vapor is condensed at test section (9), and its characteristics are measured here. The refrigerant flows through a sub-cooler (10); as a result, it becomes subcooled liquid completely, and the refrigerant flow rate is measured with a mass flow meter (11). After the joining point of the main-loop and the bypass-loop, refrigerant flows to an expansion valve (5) and an evaporator (6) in turn, it becomes superheated vapor and returns to compressor finally. The refrigerant flow rate and pressure are controlled by operating the flow control valves, expansion valve and compressor frequency.

Figure 2 shows the schematic view of the test section (top diagram) and the cross-section of test tube (bottom picture) for investigating the characteristics of R410A. The test section is composed of an inlet-mixing chamber, a multi-port extruded tube (test tube) and an outlet-mixing chamber. Test tube has 681.0mm total length and 600mm effective cooling length. Eight cooling water jackets are attached on both upside and bottom side surface of the test tube; the length of each water jacket is 150 mm. Sixteen heat flux sensors of 75mm in length are inserted in between the water jackets and the test tube. The measured heat flux with each heat flux sensor is treated as local value in the present study. Refrigerant temperature is measured with two ϕ 1.0mm K-type sheathed thermocouples inserted in the inlet mixing chamber and the outlet mixing chamber. The outer wall temperature of the test tube is measured with 16 T-type thermocouples of ϕ 76 μ m O.D. buried in the test tube at central points of every heat flux sensors. The refrigerant pressure in the mixing chamber at the inlet of the pre-cooler (8) is measured with an absolute pressure transducer. The local

pressure distribution from the inlet mixing chamber to the outlet-mixing chamber of test-section is measured through 5 pressure measuring ports using a differential pressure transducer. All of the measuring data were taken under steady-state condition. As illustrated in Figure 2 (bottom picture), the test tube is a multi-port extruded tube having 12 smooth channels of 1.12mm in hydraulic diameter.

As summarized in table 1, the experiments were carried out with a mass velocity of $G=100\sim 300(\text{kg}/\text{m}^2\text{s})$ and at a constant inlet pressure of around 2.50 MPa, while the saturation temperature of the refrigerant is



- | | |
|------------------------|---------------------------|
| (1) Compressor | (8) Pre-Heater |
| (2) Oil Separator | (9) Test Section |
| (3) Condenser | (10) Sub-Cooler |
| (4) Flow Control Valve | (11) Flow Meter |
| (5) Expansion Valve | (12) Constant Temperature |
| (6) Evaporator | Water Circulator |
| (7) Mixing Chamber | (13) Sight Glass |

Fig. 1 Schematic diagram of experimental apparatus.

about 47~51degree. The brine temperature set at a constant temperature water circulator is of -5, 5, 15 and 25 degree. The specifications of test tube are listed in table 2.

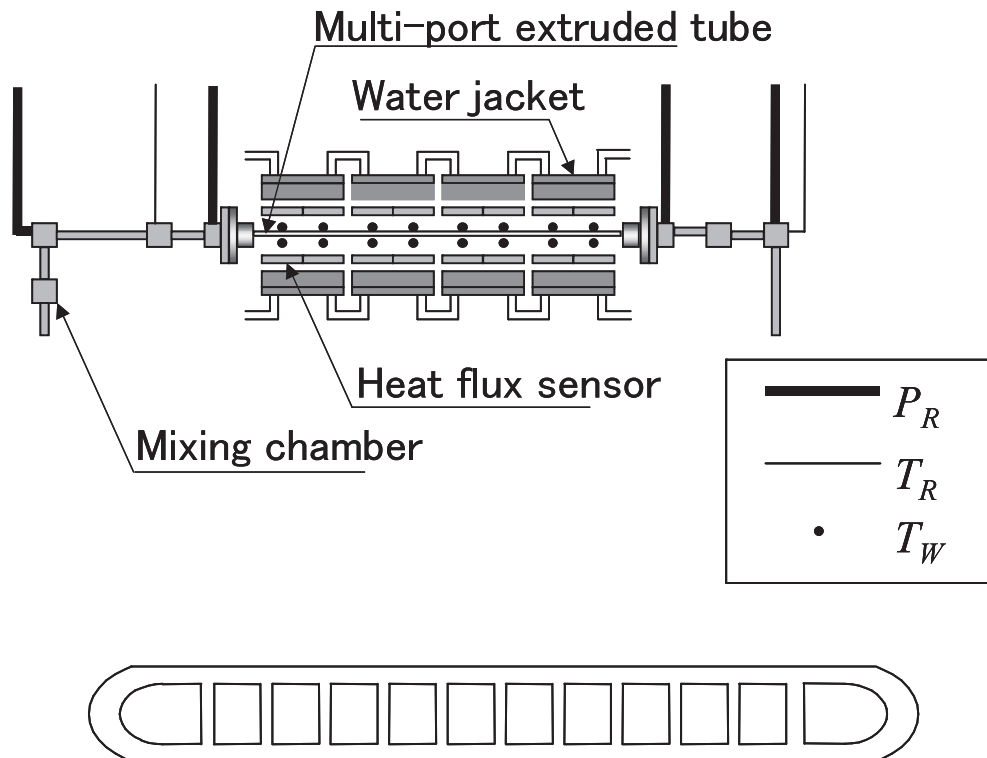


Figure 2 The schematic view of test section and cross-section of test tube

Table 1. Experimental condition

Items	Data
G [$\text{kg}/\text{m}^2\text{s}$]	100,200,300
P_{Rin} [MPa]	2.5
T_{Rin} [$^{\circ}\text{C}$]	47~51
T_s [$^{\circ}\text{C}$]	-5,5,15,25

Table 2 Specifications of test tube

Items	Data
Number of Tube Channel	12
Wetted Perimeter Length [mm]	56.60
Cross Sectional Area [mm^2]	15.83
Hydraulic Diameter [mm]	1.12
Tube length [mm]	681.0

2.2 Experimental data reduction

The following assumptions are employed in the data reduction:

- (1) In the vapor/liquid single-phase region, the pressure drop is calculated using the Colburn equation, which is employed to calculate the total pressure drop in the single-phase region and figure out the starting and ending points of condensation.
- (2) In the two-phase region, the pressure drop due to the momentum change is estimated using the homogeneous model; subtracting this pressure drop from the measured pressure drop data leads to the frictional pressure drop. (The gravitational pressure drop is neglected since the test tube is fixed horizontally.)
- (3) In a subsection where the condensation starts, the heat flux is assumed to be

- uniform in the refrigerant flow direction; this assumption is employed in order to find out the starting point of condensation.
- (4) In order to calculate the ending point of condensation, the heat flux is also assumed to be uniform in a subsection where the condensation ends
- (5) The temperatures at the inner wall of the test tube are estimated from the measured wall temperature at the outer surface of the tube by assuming one-dimensional heat conduction in the tube wall.

By solving the energy balance equation in each subsection successively in the refrigerant flow direction along with measured data of the refrigerant flow rate, the wall heat flux and the pressure, the quality change in each subsection is calculated. The local heat transfer coefficient, α , is obtained as:

$$\alpha = \frac{A_{wo}}{A_{wi}} \frac{q}{(T_R - T_{wi})} = \frac{2H}{S} \frac{q}{(T_R - T_{wi})} \quad (1)$$

where, A_{wo} is the outer cooling area of the test tube, A_{wi} is the inner cooling area of the test tube, q is the arithmetic mean of upper side and bottom side wall heat fluxes of a subsection measured by heat flux sensors, H is the width of the test tube, S is the wetted perimeter length of the test tube, T_R is the refrigerant temperature at the center of a subsection, and T_{wi} is the inner wall temperature of the test tube, and then the local Nusselt number Nu is evaluated by equation(2):

$$Nu = \frac{\alpha d}{\lambda_R} \quad (2)$$

where d is the hydraulic diameter of the test tube, and λ_R is the thermal conductivity of refrigerant liquid. In the present study, the refrigerant pressure required in order to estimate the refrigerant bulk temperature T_R is calculated with the Colburn equation in vapor or liquid single-phase region, with the correlation of Koyama et al. in two-phase region. The two-phase multiplier factor ϕ_v proposed by Koyama is shown as follows:

$$\phi_v^2 = 1 + 13.17 \left(\frac{v_L}{v_V} \right)^{0.171} \left(1 - e^{-0.6\sqrt{Bo}} \right) X_{tt} + X_{tt}^2 \quad (3)$$

Bo is Bond number expressed in terms of the ratio of the hydraulic diameter and Laplace constant, and X_{tt} is Lockhart-Martinelli parameter.

Thermophysical properties in the data reduction are referred to the REFPROP Version 7.0 [5] (McLinden et al. 1998).

3. Result and discussion

Figure 3 shows a sample that the experimental result of temperature and pressure distribution, which was carried out with a mass velocity of $G=100 \text{ kg/(m}^2\text{s)}$ and a cooling brine temperature of -6 degree. In this figure, the symbol of P_R is the refrigerant pressure at each subsection (calculated value), and $P_{R_{mix}}$ is the refrigerant pressure at the inlet and the outlet of the test section and in the mixing chambers at the inlet and the outlet of the test section (measured value); T_R is the refrigerant temperature at each subsection (calculated value), $T_{R_{mix}}$ is the refrigerant temperature in the

mixing chambers at the inlet and the outlet of the test section, respectively, and T_w is the test-tube wall temperature.

Figure 4 denotes the relation between local heat transfer coefficients α and liquid quality of refrigerant, $(1-x)$ under such conditions, namely refrigerant mass velocity $G=100, 200$ and $300 \text{ [kg/m}^2\text{s]}$, and cooling brine temperature $T_S = -5, 5, 15, 25 \text{ [}^\circ\text{C]}$.

According to figure 4, local heat transfer coefficient increases with the increase of refrigerant mass velocity. But when refrigerant mass velocity G is 100 and $200 \text{ [kg/m}^2\text{s]}$, local heat transfer coefficient has no notable difference. When refrigerant mass velocity increases from $100, 200$ to $300 \text{ [kg/m}^2\text{s]}$, to compare with free convection condensation, relatively speaking the influence of forced convection condensation strengthen. Therefore, heat transfer coefficient increases with the increase of refrigerant mass velocity.

3.1. The comparison on pressure drop between the experimental data and the correlation of Koyama et al.

Figure 5 shows the comparison between P_{exp} , the experimental data and P_{cal} , the calculated values. The calculated values of pressure drop are calculated by the correlation of Koyama et al.

The present data, P_{exp} agrees with the correlation within a deviation of $\pm 10\%$, except for the data of $G=100 \text{ [kg/m}^2\text{s]}$. In the case of $G=100 \text{ [kg/m}^2\text{s]}$, it is inferred that the measuring accuracy of the mass flow meter is lowered due to the decrease of the mass velocity. As a result, the calculated values estimated based on the measured mass flow rate have relatively large deviation compared with the case of high mass velocity.

The correlation of Koyama et al. is modified based on a correlation proposed by Mishima-Hibiki [6] (1995). One of modified measures is that replaced the item of the hydraulic diameter with Bond number. The reasonable deviation shown in Fig.5 is inferred that the Bond number is a much significant dimensionless number upon predicting the frictional pressure drop. Bond number is the ratio of the hydraulic diameter and Laplace constant implying the influence of surface tension. That's to say, the effect of surface tension is one of important factors to frictional pressure drop in mini-channel tube. In the present data reduction, the pressure drop due to the momentum change is estimated using the homogeneous model.

3.2. The comparison on local Nusselt number between experimental data and the previous correlations

Figure 6, 7 and 8 show the comparison between the experimental data of Nu number and prediction results using the correlations of Dobson et al., Cavallini et al., and Koyama et al., respectively. The present data, Nu_{exp} , agree with the correlation of Dobson within a deviation from -20% to +250%, the correlation of Cavallini within a deviation from -40% to +50%, the correlation of Koyama within a deviation from % -20% to +90%.

The heat transfer correlation of Cavallini et al., [7] (2001) which is proposed for the in-tube forced-convective condensation based on the data of relatively large diameter tubes, including the refrigerant data of R410A. In addition, Cavallini's correlation was plotted at annular flowing regime. In present study, the hydraulic diameter of test tube is around 1mm. Hence, the deviation may be inferred due to the size-reduced influence of hydraulic diameter.

The correlation of Dobson et al., [8] (1998) is plotted for R12, R22, R134a, and R32/R125. Hence the deviation may be caused by the refrigerant properties.

The correlation of Koyama et al. [1] (2002) is plotted for R134a, and both the effect of forced convection and free convection are taken into account. This correlation is over-predicted for present data. However, It may be inferred that is due to the influencing ratio of the free convection and forced convection. Owing to that the effect of the free convection is higher than that of R134a, the coefficients of the forced convection term and free convection term should be re-evaluated consequently.

4. Conclusions

The characteristics of pressure drop and heat transfer are experimentally investigated on the condensing two-phase flow of refrigerant R410A in a horizontal multi-port extruded tube. The conclusions are summarized as follow:

- (1) The correlation of Koyama et al. for frictional pressure drop agrees well with the present experimental data of R410A.
- (2) The present experimental data are also compared with the heat transfer correlation of Cavallini et al., the correlation of Dobson et al., and the correlation of Koyama et al. Those deviations are relatively large, so the empirical correlation of Nusselt number may have some possibility to be modified

and a better correlation be looked forward.

To establish a predicting method of the pressure drop and heat transfer characteristics of refrigerant condensing in a small diameter tube, experimental data should be more accumulated and the following terms should be considered: (1) flow pattern, (2) the surface tension due to reduced-size hydraulic diameter in mini-channel tube, and (3) the weights of the forced convection and the free convection terms in a correlation of Nusselt number due to refrigerant working-pressure and properties.

Acknowledgement

Financial support and the experimental apparatus assembled from Mitsubishi Electric Corporation are kindly acknowledged, here.

References

- 1 Koyama, S., Kuwahara, K. and Nakashita, K., 2003, Condensation of Refrigerant in a Multi-port Channel, Proc. of First International Conference on Microchannels and Minichannels, Rochester, New York, U.S.A, 193-205.
- 2 Yang, C-Y., Webb, R. L., 1996, Condensation of R-12 in Small Hydraulic Diameter Extruded Aluminum Tubes with and without Micro-Fins, Int. J. Heat Mass Transfer, Vol.39: 791-800.
- 3 Katsuta, M., 1994, The Effect of a Cross-Sectional Geometry on the Condensation Heat Transfer Inside Multi-Pass Tube, Proc. WTPF, POSTECH, Vol.2: 146-157.
- 4 Moser, K. W., Webb, R. L. and Na, B., 1998, A New Equivalent Reynolds Number Model for Condensation in Smooth Tubes, ASME J. Heat Transfer, Vol.120: 410-417.
- 5 McLinden, M. O., Klein, S. A., Lemmon, E. W., Peskin A. P., 2002, *NIST thermodynamic properties of refrigerants and refrigerant mixtures database* (REFPROP), Ver. 7.0.
- 6 Mishima, K., Hibiki, T., 1995, Effect of inner diameter on some characteristics of air-water two-phase flows in capillary tubes, Trans. JSME, (B): 61-589,99-106 (in Japanese).
- 7 Cavallini, A., Censi, G., Delcol, D., Doretto, L., Rossetto, L., 2001, Condensation Heat Transfer in Annular Flow: A New Predictive Model for Pure Fluids, IIR Conference, Paderborn, B1.27-B1.34.
- 8 Dobson, M.K., Chato, J.C., 1998, Condensation in Smooth Horizontal Tubes, *Journal of Heat Transfer, Transactions of the ASME*, Vol.120: 193-213.

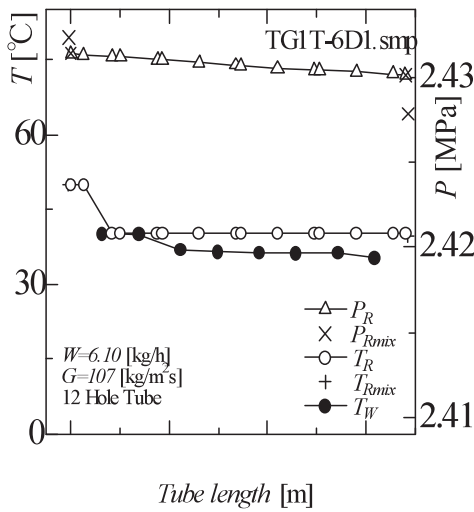


Figure 3 The Distributions of Temperature and Pressure at experiment condition of $G=100 [kg / m^2 s]$ and $T_s=-6^\circ C$

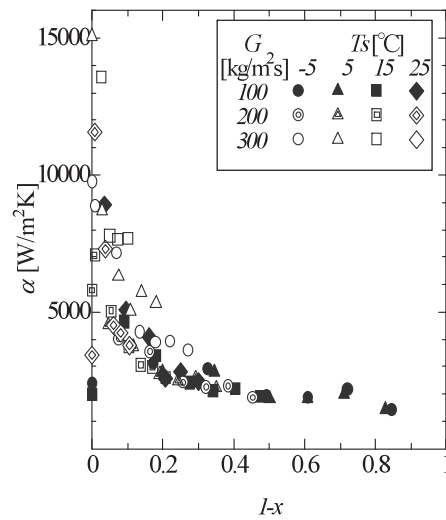


Figure 4 The Distributions of heat transfer coefficient vs. refrigerant quality

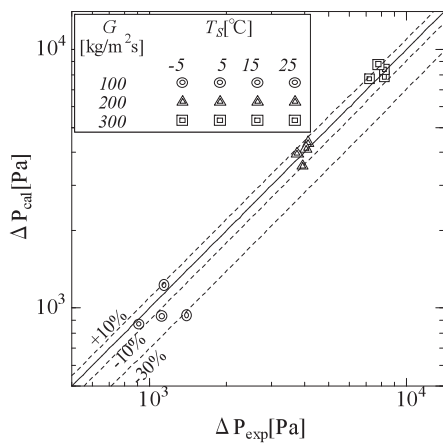


Figure 5 Comparison of pressure drop between the experimental data and Koyama correlation

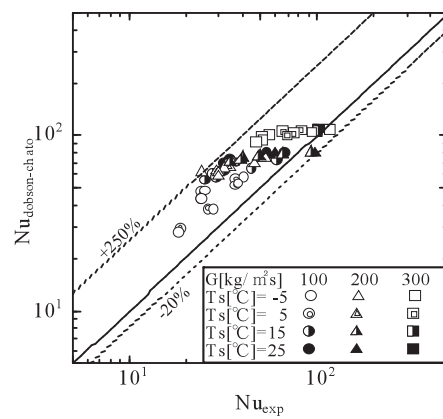


Figure 6 Comparison of Nu between the experimental data and the correlation of Dobson *et al.*

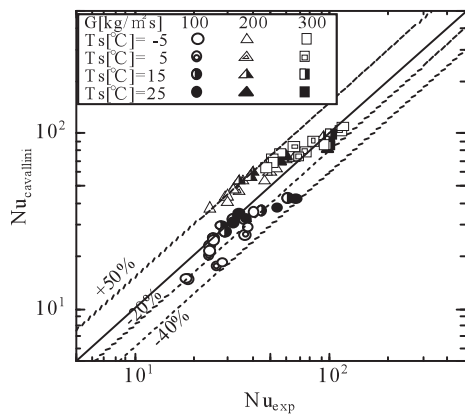


Figure 7 Comparison of Nu between the experimental data and the correlation of Cavallini *et al*

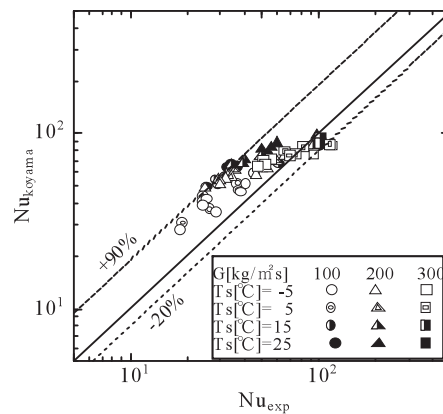


Figure 8 Comparison of Nu between the experimental data and the correlation of Koyama *et al*

Nomenclature

A	Area	[m ²]	Bo	Bond number	[-]
d	Hydraulic diameter of test tube	[m]	G	Mass flux	[Kg/(m ² s)]
H	Width of the test tube	[m]	Nu	Nusselt number	[-]
P	Pressure	[MPa]	q	Heat flux	[KW/m ²]
S	Wetted perimeter length of test tube	[m]	T	Temperature	[K]
α	Heat transfer coefficient	[W/(m ² K)]	λ	Thermal conductivity	[W/(m k)]
ν	Kinematic viscosity	[m ² s]	ϕ	Two-phase multiplier factor	[-]
Xtt	Lockhart-Martinelli parameter	[-]			
			Subscript		
L	Liquid of refrigerant	[-]	R	Refrigerant	[-]
V	Vapor of refrigerant	[-]	wi	Inner surface of test tube	[-]
wo	Outer surface of test tube	[-]			